Effects of low-frequency noise in driven coherent nanodevices

2012 Phys. Scr. 2012 014020

(http://iopscience.iop.org/1402-4896/2012/T151/014020)

Phys. Scr. **T151** (2012) 014020 (8pp) doi:10.1088/0031-8949/2012/T151/014020

Effects of low-frequency noise in driven coherent nanodevices

G Falci[1,2], M Berritta[3], A Russo[3], A D'Arrigo[2,3] and E Paladino[1,2]

[1] Dipartimento di Fisica e Astronomia, Università degli Studi Catania and Centro Siciliano di Fisica Nucleare e Struttura della Materia (CSFNSM), Via Santa Sofia 64, I-95123 Catania, Italy
[2] CNR-IMM MATIS, Consiglio Nazionale delle Ricerche, Via Santa Sofia 64, I-95123 Catania, Italy
[3] Dipartimento di Fisica e Astronomia, Università degli Studi Catania, Via Santa Sofia 64, I-95123 Catania, Italy

E-mail: gfalci@dmfci.unict.it

Received 12 September 2012
Accepted for publication 18 September 2012
Published 30 November 2012
Online at stacks.iop.org/PhysScr/T151/014020

Abstract
We study the effect of low-frequency noise in ac-driven two- or many-level coherent nanodevices. Fluctuations in the properties of the device are translated into equivalent fluctuations of the driving fields. The impact on Rabi oscillations can be modulated with the detuning and minimized at resonance. In three-level atoms slow noise produces qualitative changes for protocols as coherent population transfer. We propose a strategy allowing us to operate at parity symmetry points, where the device is well protected against noise, despite selection rules preventing direct couplings to external fields of involved transitions.

PACS numbers: 03.67.Lx, 85.25.-j, 03.65.Yz

(Some figures may appear in color only in the online journal)

1. Introduction

Quantum dynamics of solid-state nanosystems is nowadays a fertile subject of investigation which has been boosted over the last decade by research towards the implementation of quantum state processors [1]. Nanodevices behaving like artificial atoms have allowed demonstration on a mesoscopic scale of coherent phenomena proper of the microscopic realm. Advances in fabrication offer a possibility of exploring several different designs of quantum bits based on semiconductors and superconductors [2–4]. In the latter, mechanisms and typical features of decoherence [4–6] are now well understood and several strategies for minimizing them have been tested. This has allowed fabrication of more complex architectures which in particular have demonstrated quantum optics on a chip [7] and to stimulate the exploration of new designs beyond atomic analogues. To proceed in this direction, quantum control of coherence in driven superconducting multilevel open nanostructures has to be achieved. A key step is understanding how peculiar signatures of interference, such as those exhibited in driven multilevel systems [8], are sensitive to the presence of environments unconventional [9] in atomic physics.

Artificial atoms [10] are different from their natural counterpart in many respects. Indeed, their properties can be engineered and are easily tunable. The impact on one of the major issues of coherent dynamics, namely resilience to noise, is large and has been exploited in a twofold way. First of all, devices can be tuned to optimal bias points where symmetries enforce protection from decoherence [11–13]. On the other hand, the possibility of manipulating various external knobs allows us to extract valuable information on the sources of decoherence. In recent years, environment spectroscopy techniques that use as meters both undriven and driven (pulsed or continuously) coherent nanodevices have been developed [15–19]. Nanodevices offer the possibility of designing couplings, with external fields or between subunits, which are much stronger than what is found in atomic systems [7]. Therefore they may allow for faster operation, but on the other hand, noise may be large, determining smaller decoherence times.

We stress that the relation between tunability and resilience to noise has special significance for solid-state nanodevices because of the central role played by low-frequency noise in determining dephasing [5, 6, 20]. Indeed, the sensitivity of qubit performances both to fabrication parameters, whose fluctuations represent a major issue in the scalability of the architectures, and to external bias, whose fluctuations act as stray parameters during the operations, is well known.

In this work, we focus on the effects of low-frequency noise in driven systems, with the goal of both maximization of the efficiency of external controls and enhancement of protection against noise. These are often conflicting requirements; therefore it must be understood how is the tradeoff optimized. In section 2, we derive a phenomenological Hamiltonian starting from the general model of a noise-driven nanodevice and state the approximations to be used subsequently. In section 3, we study the effect of low-frequency noise on a driven two-level nanodevice. In section 4, we discuss the qualitative impact of low-frequency noise and the role of selection rules in the implementation of a conventional protocol for coherent population transfer in nanodevices, and in section 5, we propose a new scheme allowing us to operate at a symmetry-protected working point.

2. Model for driven noisy quantum devices

We start from the macroscopic Hamiltonian of the device, $H_0 = H_0(q)$, which is an operator onto an n-dimensional Hilbert space $\mathbb{H}$. It depends on the parameter q fixing the bias (operating) point. The 'local' basis of $\mathbb{H}$ is composed of the eigenstates $\{|\phi_i(q)\rangle : i = 1, \ldots, n\}$ of $H_0(q)$. In this 'laboratory frame' the Hamiltonian is

$$H_0 = \sum_{i=1}^{n} E_i(q)\, |\phi_i(q)\rangle\langle\phi_i(q)|. \tag{1}$$

External control is described by a time-dependent term. In a one-port design the driving field $A(t)$ couples to a single time-independent system operator $\hat{Q}$

$$H_c(t) = A(t)\, \hat{Q}, \tag{2}$$

which is Hermitian and traceless. In general, control is operated via the same port, i.e. by allowing the bias in $H_0(q)$ to depend on time. We let $q \to q(t) + q_c(t)$, splitting it into a slow $q(t)$ which includes static bias, and the fast control parameter $q_c(t)$. Accordingly, we split

$$H_S = H_0[q(t) + q_c(t)] := H_0[q(t)] + H_c(t), \tag{3}$$

where $H_c(t)$ describes (fast) control; in relevant situations it can be linearized in $q_c(t)$, yielding the structure of equation (2). Note that while $\hat{Q}$ is an observable and does not depend on the local basis, its matrix representation does. The physical consequence is that the effectiveness of the fast control $q_c(t)$ in triggering transitions depends also on the slow $q(t)$, a feature of artificial atoms reflecting their ease of tunability.

The interaction with the complicated environment of microscopic degrees of freedom in the solid state can be modeled by a phenomenological Hamiltonian. We first consider classical noise and assume that it also acts through the same control port; therefore it can be modeled by adding a stochastic component $x(t)$ to the drive. Again we split slow and fast noise, $x(t) \to x(t) + x_f(t)$, and include the slow part in H_0. The same steps leading to equation (3) yield the noisy Hamiltonian

$$H = H_0[q(t) + x(t)] + A(t)\, \hat{Q} + H_{nf}, \tag{4}$$

where H_{nf} describes Markovian high-frequency classical noise. 'Quantization' of this term, $H_{nf}(t) \to \hat{X}\, \hat{Q} + H_R$, yields the final system–environment Hamiltonian. Here $\hat{X}$ operates on the environment and H_R is its Hamiltonian, plus possibly suitable counterterms.

From the physical point of view, the phenomenological Hamiltonian treats on different footings environmental modes exchanging energy with the system, which are treated quantum mechanically, and slow modes responsible for pure dephasing, which are accounted for classically. The results of measurements involve both quantum and classical ensemble averaging. From a technical point of view, the effects of Markovian noise alone are studied by weak coupling quantum optical master equations. This approach fails for low-frequency noise (e.g. $1/f$), which is large in solid-state systems. To overcome this problem, a multistage approach has been proposed [20] for undriven systems subject to broadband noise, which quantitatively explains the decoherence observed in superconducting qubits of different nature [15, 18, 19]. In these cases the leading contribution of low-frequency noise was captured by a static-path approximation (SPA), i.e. approximating $x(t)$ by a suitably distributed random variable x [15, 20]. Despite its simplicity, this approximation provides a powerful framework for applications to more complex architectures. In recent years, it has been used to propose a design of optimal tuning of multiqubit systems [12, 13] and extended to the analysis of a Λ system [14]. An important feature of superconducting nanodevices is that the Hamiltonian $H_0[q]$ can be tuned in such a way that parity symmetries are enforced where $A_i \equiv \partial E_i/\partial q = 0$ and selection rules hold affecting the matrix elements Q_{ij} in the local basis. In these parity symmetry points, the device is well protected against noise.

In this work, we will study ac-driven nanodevices addressing the effects of low-frequency noise in the SPA. We will focus on the single-port scheme where control, noise and environmental modes all couple to the same operator $\hat{Q}$. Now, it is apparent that different channels for decoherence will be strongly correlated: this has consequences for quantum control. The single-port scheme provides the simplest model displaying these features, and at the same time it describes experimentally relevant devices affected by a dominant source of decoherence. A more general multiport scheme would exhibit an even richer behavior of correlation, whose essence stems from the non-Markovianity of noise.

3. ac-driven two-state systems

We model a nanodevice in an external ac field by the Hamiltonian

$$H(t|x) = H_0[q + x] + A(t)\, \hat{Q}, \tag{5}$$

where $A(t) = \mathcal{A} \cos\phi(t)$ is the control field with carrier frequency ω. The device is nominally biased at q with a random additive component x distributed with a zero average $\mathcal{P}(x)$. We consider $H_0[q + x]$ and for each x we define (dependence on q is omitted hereafter) the 'x-basis' $\{|\phi_i(x)\rangle\}$ of its eigenstates and the conditional (Schrödinger or laboratory frame) propagator $U_S(t|x)$

corresponding to $H(t|x)$. Usual protocols in nanodevices start with an imperfect (x-dependent) initialization in the lowest energy state, $\rho(0) = \int \mathrm{d}x \mathcal{P}(x)\, |\phi_0(x)\rangle\langle\phi_0(x)|$. Then the system evolves conditionally to x as $\rho(t|x) = U_S(t|x)\ |\phi_0(x)\rangle\langle\phi_0(x)|\ U_S^\dagger(t|x)$. Finally, populations of the x-dependent eigenstates are measured, yielding

$$P_i(t) = \int \mathrm{d}x\, \mathcal{P}(x)\, \langle\phi_i(x)|\rho(t|x)|\phi_i(x)\rangle, \tag{6}$$

i.e. the simple ensemble average of conditional population histories. Averaging defocuses the coherent signal, which appears to be suppressed in time. Alternative preparations and readout of different observables may lead to further suppression of the signal, which however does not accumulate in time. In these cases equation (6) is not exact, but it is still a good approximation.

We now derive $U_S(t|x)$ in the rotating wave approximation (RWA). To this end, we represent in the x-basis, $H_c(t) = A(t)\,\hat{Q} = \sum_{ij} A(t) Q_{ij}(x)$, and approximate this control Hamiltonian by retaining only off-diagonal quasi-resonant entries, Q_{ij} such that $|E_i - E_j| \sim \omega$, and by neglecting the counter-rotating part of the field. If only the lowest doublet is addressed, this yields

$$H_{RW}(t|x) = \frac{\mathcal{A}}{2}\, \mathrm{e}^{-\mathrm{i}\phi(t)}\ Q_{10}(x)\ \hat{P}_{10}(x) + \mathrm{h.c.},$$

where $\hat{P}_{ij}(x) = |\phi_i(x)\rangle\langle\phi_j(x)|$ are the transition operators. Physically, the RWA keeps only control entries 'effective' in triggering transitions between different states. Note that this effective part of the control depends on the random variable x. Terms we neglect produce a small shift in the frequencies and a small fast modulation of the signal.

3.1. Rabi oscillations

Rabi oscillations are studied in a rotating frame (RF) obtained by the unitary transformation $U_{rf}(t|x) = \mathrm{e}^{-\mathrm{i}\phi(t)\hat{P}_{11}(x)}$, such that $U_S(t|x) = U_{rf}(t|x)\, U(t|x)$, $U(t|x)$ being the propagator in the RF. The transformation does not affect population histories, equation (6); therefore we only need $U(t|x)$ given by the corresponding RF Hamiltonian. The relevant dynamics is described by the restriction onto the $\{|\phi_i(x)\rangle,\ i = 0, 1\}$ subspace, which reads

$$\tilde{H}(t|x) = \begin{bmatrix} 0 & \Omega_R^*(x)/2 \\ \Omega_R(x)/2 & \delta(t|x) \end{bmatrix}. \tag{7}$$

Here $\Omega_R(x) = \mathcal{A}\, Q_{10}(x)$ is the peak Rabi frequency and $\delta(x) = E_1(x) - \omega$ is the detuning for a monochromatic field $\dot{\phi}(t) = \omega$ (we let $E_0 = 0$). Note that the effect of low-frequency noise in artificial atoms, which is due to their internal fluctuations, is conveniently recast in terms of sensitivity to imperfections (both in phase and in amplitude) of a fictitious drive. The corresponding populations are readily found, e.g. $P_1(t|x) = \Omega_R/(2\Omega_{fl})\,[1 - \cos(\Omega_{fl} t)]$ where the flopping frequency for Rabi oscillations is $\Omega_{fl}(x) = \sqrt{\delta^2(x) + \Omega_R^2(x)}$. The average, equation (6), yields

$$P_1(t) = \bar{P}_1 - \bar{P}_1\, \mathcal{R}e\langle \mathrm{e}^{-\mathrm{i}\Omega_{fl}(x)t}\rangle,$$

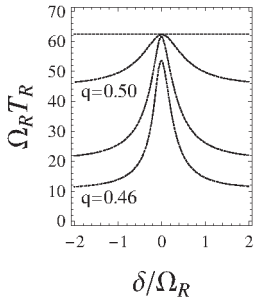

Figure 1. Decay time T_R of Rabi oscillations (obtained from $\mathcal{I}m\ \Phi(T_R) = -1$) as a function of the nominal detuning δ_0 for a CPB in the charge regime. The curve $q = 0.5$ refers to the symmetry point, whereas the others $q = 0.48,\ 0.46$ refer to the devices biased off-symmetry. The top line $T_R = \mathrm{const} = 2/\gamma$ is the decay time for spontaneous emission which is added to each curve.

where we neglected amplitude fluctuations, approximating $\bar{P}_1 \approx \Omega_{R0}/\sqrt{\delta_0^2 + \Omega_{R0}^2}$ with values at $x = 0$ (still depending on the bias q). This requires small x-induced fluctuations of the Rabi couplings and of the level splitting. Under the same conditions we can calculate the average by expanding to second order $\Omega_{fl}(x) \approx \Omega_{fl}(0) + Ax + \frac{1}{2}Bx^2$, and assuming that $\mathcal{P}(x)$ is a Gaussian with variance σ_x, obtaining

$$\langle \mathrm{e}^{-\mathrm{i}\Omega_{fl}(x)t}\rangle = \mathrm{e}^{-\mathrm{i}\Omega_{fl}(0)t}\ \mathrm{e}^{-\mathrm{i}\Phi(t)} \tag{8}$$

$$\mathrm{e}^{-\mathrm{i}\Phi(t)} = \frac{1}{\sqrt{1 + \mathrm{i}B\sigma_x^2 t}}\ \exp\left[-\frac{A^2\sigma_x^2 t^2}{2(1 + \mathrm{i}B\sigma_x^2 t)}\right]. \tag{9}$$

This equation describes different regimes for the decay of Rabi oscillations, namely a Gaussian time decay $|\mathrm{e}^{-\mathrm{i}\Phi(t)}| \sim \mathrm{e}^{-\frac{1}{2}A^2\sigma_x^2 t^2}$ when the linear term in the expansion dominates, and power-law behavior $\sim 1/(\sigma_x\sqrt{Bt})$ when $A \to 0$. In this regime, equation (9) describes the initial suppression of the signal. On longer time scales in fact, physical systems usually decay exponentially, $\sim |\mathrm{e}^{-\mathrm{i}\Phi(t)}|\, \mathrm{e}^{\gamma t/2}$, due to spontaneous decay processes with rate γ, not accounted for in the SPA.

The important point is that the coefficients of the expansion depend on several parameters, as $A = A(q, q_c, \delta_0)$, where q_c is the amplitude of the control and δ_0 the nominal detuning (see the appendix). Since they are tunable, a systematic investigation can be made. Further information needed, i.e. the dependence on q of the energy spectrum, and of matrix elements $Q_{ij}(q)$, comes from the characterization of the device. The choice[4] of a Gaussian $\mathcal{P}(x)$ can be physically motivated and its variance can be related to the integrated power spectrum of low-frequency noise, $\sigma_x = \int (\mathrm{d}\omega/\pi)\langle x\, x\rangle_\omega$ [5, 20]. This information can be extracted from free induction decay or Ramsey experiments [15, 19]; therefore equation (9) can be checked with no free parameters.

Note that even if equation (9) describes the same regimes of the SPA for coherent oscillations of undriven systems [20], here the situation is different. In particular, equation (9) quantitatively accounts for the fact that ac driving greatly reduces decoherence compared to undriven systems. This is a common statement based on the intuitive expectation

[4] For more general distributions the average in equation (9) can be calculated with the steepest descent method, yielding, for small enough σ_x, a result with the same structure.

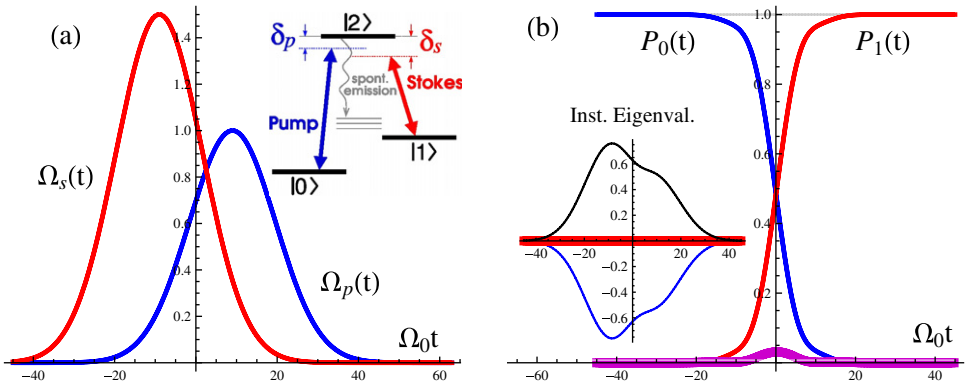

Figure 2. STIRAP in a three-level system ($|\phi_i\rangle \equiv |i\rangle$). (a) Pulses in a counterintuitive sequence, the Stokes field being switched on *before* the pump field (here $\Omega_0 = \Omega_p$ fixes the scale, $\kappa = \Omega_s/\Omega_p = 1.5$ and the reduced pulse width is $\Omega_0 T = 15$); in the inset the Lambda configuration. (b) Population histories for nearly ideal STIRAP: population starts in $|\phi_0\rangle$ ($P_0(-t_0) = 1$) and ends in $|\phi_1\rangle$ ($P_1(t_0) = 1$), while $|\phi_2\rangle$ is almost never populated; in the inset the instantaneous eigenstates, the dark state corresponding to the zero eigenvalue.

that an ac field may average effects of noise, as corroborated by experiments [15]. To be more specific, let us neglect, for the moment, fluctuations of Q_{ij}. At resonance, $\delta_0 = 0$, non-vanishing linear fluctuations of the spectrum, $A_1 \neq 0$, determine quadratic fluctuations of $\Omega_{\rm fl}(x)$. Therefore $A = 0$ and Rabi oscillations undergo power-law decay, whereas in the absence of drive they determine the much stronger Gaussian decay $\sim {\rm e}^{-\frac{1}{2}A_1^2\sigma_x^2 t^2}$ of coherent oscillations. In this regime, measurements of Rabi oscillations [18] have been used to probe the environment[5] of a flux qubit. At symmetry points, where $A_1 = 0$, coherent oscillations decay with a power law, whereas Rabi oscillations are practically unaffected by low-frequency noise, and in physical systems they decay only due to spontaneous emission.

Exploiting the dependence on the detuning, we find that for non-vanishing δ_0 the decay laws are the same as those for coherent oscillations (figure 1). In particular at symmetry points low-frequency noise determines an initial decoherence which takes over spontaneous decay. An even stronger suppression of coherence occurs off-symmetry. Therefore for increasing δ_0 we expect dephasing to interpolate between the behaviors of ac-driven and undriven systems, all the phenomenology depending on the single noise figure σ_x.

The above picture is applicable to many physical situations, since fluctuations of Q_{ij} are small. Indeed, they correspond to a fraction of $\Omega_{\rm R} \neq 0$, whereas $\delta(x)$ fluctuates on the scale of the Bohr splitting $E_1 - E_0 \gg \Omega_{\rm R}$ and may be particularly relevant for $\delta_0 = 0$. However, the dependence $Q_{ij}(q)$ may lead to consequences for multilevel systems. We will come back to this point in the conclusions.

4. Coherent population transfer

We now apply the approach of the last section to driven three-level systems whose coherent dynamics clearly displays new beautiful interference phenomena [8] when addressed by two laser fields quasi-resonant with two of the three transition energies. Several protocols have been suggested for artificial atoms which may help overcome difficulties in performing certain tasks, related to the precise shaping of the pulses in the presence of imperfections ([21] and references therein). Related examples are electromagnetically induced transparency [22] and population transfer between given states [23–26], which may be implemented by using two-tone pulses in the Lambda configuration (figure 2(a)) $A(t) = \mathcal{A}_{\rm p}(t)\,\cos\phi(t) + \mathcal{A}_{\rm s}(t)\,\cos\phi_{\rm s}(t)$. The effective Hamiltonian is obtained starting from equation (5) and retaining in the control part only quasi-resonant entries in the RWA

$$H_{\rm RW}(t|x) = \frac{1}{2}\Big[\mathcal{A}_{\rm p}\,{\rm e}^{-{\rm i}\phi_{\rm p}(t)}\,Q_{20}(x)\,\hat{P}_{20}(x) + \mathcal{A}_{\rm s}\,{\rm e}^{-{\rm i}\phi_{\rm s}(t)}\,Q_{21}(x)\,\hat{P}_{21}(x)\Big] + {\rm h.c.} \qquad (10)$$

Then we define a doubly RF by the transformation $U_{\rm rf}(t|x) = {\rm e}^{{\rm i}[\phi_{\rm p}(t)\hat{P}_{00}(x) + \phi_{\rm s}(t)\hat{P}_{11}(x)]}$ and project onto the lowest three-level (x-dependent) subspace, obtaining

$$\tilde{H}(t|x) = \begin{bmatrix} 0 & 0 & \Omega_{\rm p}^*(t)/2 \\ 0 & \delta(x) & \Omega_{\rm s}^*(t)/2 \\ \Omega_{\rm p}(t)/2 & \Omega_{\rm s}(t)/2 & \delta_{\rm p}(x) \end{bmatrix}, \qquad (11)$$

where $\delta(x) = E_1(x) - (\omega_{\rm p} - \omega_{\rm s})$ is the two-photon detuning, $\delta_{\rm p}(x) = E_2(x) - \omega_{\rm p}$ is the pump pulse detuning and $\Omega_i(t)$ are pulses of width T and peak Rabi frequency $\Omega_{\rm p} = Q_{02}\,A_{\rm p}$ and $\Omega_{\rm s} = Q_{12}\,A_{\rm s}$, respectively.

In the ideal STIRAP ([27] and references therein; [28]), the protocol is carried at two-photon resonance, $\delta = 0$, and in this case the system is trapped in a 'Dark state'. By shining pulses in the counterintuitive sequence (figure 2(a)) the dark state evolves adiabatically from $|\phi_0\rangle$ to $|\phi_1\rangle$ implementing faithful and selective coherent population transfer (figure 2(b)), a procedure named the stimulated Raman adiabatic passage (STIRAP). Adiabaticity is enforced by the opening of field-induced Autler–Townes (AT) splittings between instantaneous eigenstates.

The model Hamiltonian equation (11) has been used to study the implementation of a Lambda configuration in superconducting devices based on the Cooper pair box (CPB) design in the presence of low-frequency noise [14, 29]. Several theoretical proposals [21, 23, 25] pointed out that close to symmetry points the pump coupling is very small due

[5] In this case, the noise source and drive were not referring to the same port; the results of this work can be easily extended to devices with many noise ports.

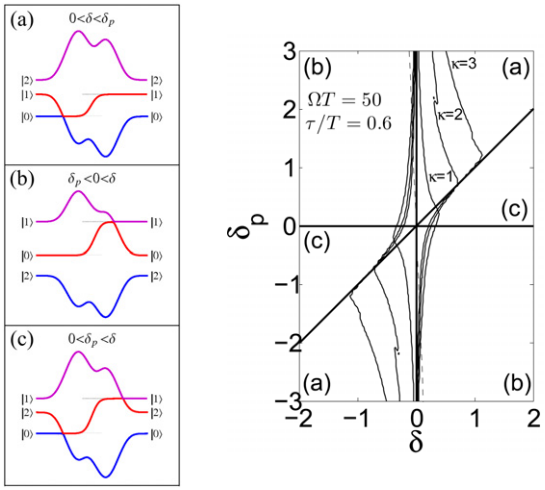

Figure 3. Left panel: typical LZ patterns with one crossing in the Stokes-AT phase, one crossing in the pump-AT phase and two crossings. Right panel: efficiency diagram $P_1(t_f)$ versus the detunings. The configurations (δ, δ_p) determine the typical LZ pattern as indicated in the regions of the phase diagram. By increasing the Stokes field amplitude (increasing κ) the efficiency in region (a) increases, minimizing the effect of the corresponding avoided crossing.

to selection rules; therefore the device must be biased slightly off-symmetry. As a consequence, decoherence increases and optimization of the tradeoff between efficient coupling and protection against low-frequency noise is necessary [14].

In what follows, we discuss a striking consequence of non-Markovianity of noise emerging already at the SPA level, namely that correlation between energy fluctuations are important since they qualitatively affect population transfer and possible control strategies to increase the efficiency.

While fluctuations of the energy spectrum of the device appear as random detunings, in equation (11) we have omitted fluctuations of Ω_i induced by the random $Q_{ij}(x)$, as suggested by the argument of section 3. Indeed, a detailed theoretical analysis for the CPB design [29] has shown that STIRAP is successful only for a bias (off-symmetry) such that energy fluctuations are linear in x and the dependence $Q_{ij}(x)$ is slow. Fluctuations of $Q_{20}(x)$ are important only closer to the symmetry point [29], where however STIRAP is already prevented by selection rules.

The mapping of energy fluctuations onto $\delta(x)$ allows us to translate to solid-state devices several results from the quantum optics realm. For instance, the well-known critical sensitivity to two-photon detuning [28] implies that the main figures to be minimized for efficient population transfer in nanodevices are fluctuations of the lowest energy splitting, E_1. This is the same requirement for the two-state system to efficiently work as a qubit. Non-zero δ modify the whole adiabatic picture of STIRAP [28] since the dark state is no longer an instantaneous eigenstate and there is no adiabatic connection from the initial to the target state. However, non-ideal STIRAP may still take place via non-adiabatic transitions between adiabatic states. For small values of δ, narrow avoided crossings between instantaneous eigenvalues occur and the population is transferred by the Landau–Zener (LZ) tunneling [27, 28] (see figure 3). Increasing δ reduces the transfer efficiency and, in general, the excited state $|\phi_2\rangle$ is populated during the protocol.

Non-adiabatic LZ patterns for STIRAP can be classified into three categories, namely: (a) a single (avoided) crossing is present at the beginning (Stokes-AT phase) of the protocol; (b) one crossing at the end (pump-AT phase); (c) two crossings, one in each phase (see figure 3, left panel). Each category corresponds to a specific relation between the detunings, e.g. pattern (b) is obtained for anticorrelated detunings $\mathrm{sign}(\delta) = -\mathrm{sign}(\delta_p)$, as illustrated in figure 3(b). This correspondence can be understood by inspection of the eigenvalues in the AT phases. For instance, during the pump-AT phase $\Omega_s = 0$, the energy δ of $|\phi_1\rangle$ is constant, whereas $\Omega_p \neq 0$ determines further splitting (AT effect) between $|\phi_0\rangle$ and $|\phi_2\rangle$ which disappears at the end of the protocol.

This classification finds a physical realization in nanodevices since detunings are not independent, the corresponding energy fluctuations reflecting the behavior of the spectrum as a function of the bias parameter q. For instance, in CPB's charge, noise determines anticorrelated fluctuations of detunings, and LZ pattern (b), whereas fluctuations of the Josephson energy would determine correlated detunings, and LZ patterns (a).

Since efficient STIRAP requires large LZ tunneling, a way to minimize the effect of stray detunings is to use, if possible, fields with larger amplitude closing the gap between avoided crossings. In particular, a larger Ω_s increases the efficiency for patterns (a) and a larger Ω_p for patterns (b). In figure 3 (right panel), it is shown how a larger Ω_s, which is not suppressed by selection rules, may widen the stability region against correlated fluctuations (a) of the detunings.

In general, specific strategies to increase the efficiency depend on the properties of the band structure, such as correlations of the parametric fluctuations of the splittings. From a different point of view, this result suggests that a proper band structure may be engineered where effects of noise can be dynamically minimized by the available control. It is worth stressing that this picture relies on correlations enforced by the non-Markovianity of noise. Indeed, pure dephasing due to Markovian processes determines a loss of efficiency which does not depend on the external fields and therefore cannot be dynamically suppressed [30].

5. STIRAP at a symmetry point

A careful study demonstrated the possibility to realize a Lambda configuration allowing for STIRAP implementation in a superconducting device such as the CPB biased off-symmetry, in the presence of broadband noise [29]. However, the efficiency would be strongly limited and noise correlations arising from the band structure might be reduced only employing far too large pump pulses. The same is true for flux qubit.

In the following, we propose an implementation of the Lambda scheme at the symmetry point where energy fluctuations are greatly reduced. Since the pump field cannot be directly coupled to the transition, we seek two-photon pump coupling. To this end, we address the three-level system by a three-tone drive (figure 4(a)) $A(t) = \sum_k \mathcal{A}_k(t) \cos \phi_k(t)$.

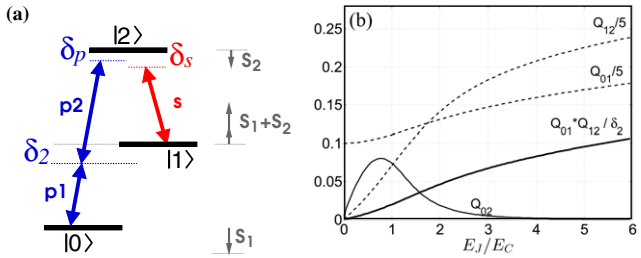

Figure 4. (a) Lambda scheme with a two-pump fields (p_1,p_2) providing an effective (0, 2) two-photon pump coupling, but producing in addition Stark shifts (S_1,S_2) of the undriven levels. (b) Off-diagonal matrix element of a CPB as a function of E_J/E_C. Matrix elements Q_{01} and Q_{12} (divided by 5) are large at the symmetry point, therefore the effective coupling $\propto Q_{01}Q_{12}/\delta_2$ is large enough and increases with E_J/E_C. In contrast, Q_{02} (here off-symmetry) is non-monotonic.

Here $k = s$ labels a component with carrier frequency close to the Stokes transition, whereas $k = p_1$, p_2 refers to two drives implementing two-photon Rabi oscillations [28] at the pump transition, $|\phi_1\rangle$ being the intermediate level (figure 4). Thus the drives $k = p_1$, p_2 must couple $|\phi_1\rangle$ in the dispersive regime, i.e. their carrier frequencies ω_k must be sufficiently detuned from resonance. If we define $E_1 - \omega_{p1} = \delta_2$ and $E_2 - E_1 - \omega_{p2} = \delta_p - \delta_2$, the condition is $\Omega_k \ll |\delta_2|, |\delta_p - \delta_2|$. The dispersive coupling ensures that $|\phi_1\rangle$ is not populated by the pump pulse. Rabi frequencies and detuning must of course be much smaller than the corresponding bare level splittings. Neglecting the Stokes field, we write the RW Hamiltonian in a doubly RF defined by $U_{rf}(t) = e^{i[\phi_{p1}(t)\hat{P}_{00} - \phi_{p2}(t)\hat{P}_{22}]}$

$$\tilde{H}_p = \begin{bmatrix} 0 & \Omega_{p1}^*/2 & 0 \\ \Omega_{p1}/2 & \delta_2 & \Omega_{p2}^*/2 \\ 0 & \Omega_{p2}^*/2 & \delta_p \end{bmatrix}. \qquad (12)$$

An effective Hamiltonian, which captures the coarse-grained dynamics over times Δt such that $\Omega, \delta \ll 1/\Delta t \ll |E_i - E_j|$, can be obtained by adiabatic elimination, considering that in the dispersive regime the intermediate level is effectively uncoupled, and accounting for its Stark shift in second-order perturbation theory, which leads to an intuitive result shown in figure 4. The effective Hamiltonian can also be obtained employing the average Hamiltonian theory [31, 32]. This approach also shows that the Stokes pulse adds independently to the effective Hamiltonian at the same level of coarse graining. This statement is valid provided the individual pump pulses are in the dispersive regime, which is relevant for STIRAP, even when $|\phi_1\rangle$ is populated. Based on these considerations, the RWA Hamiltonian for the three-photon Lambda scheme is obtained by adding to equation (12) the Stokes pulse Hamiltonian $\tilde{H}_s$, $\tilde{H}_s = \frac{1}{2}\left[\Omega_s(t)\, e^{-i\phi(t)}\, |2\rangle\langle 1| + \text{h.c.}\right]$, where $\phi(t) = \phi_s(t) - \phi_{p_2}(t)$. The phase is related to detunings $\dot{\phi}(t) = \delta(t) - \delta_2(t)$; thus it is slowly varying, as well as $\Omega_s(t)$. The coarse-grained version of the Hamiltonian is

$$\tilde{H} \approx \tilde{H}_{ave} = \begin{bmatrix} S_1 & 0 & \Omega_p^*/2 \\ 0 & \delta_2 - (S_1 + S_2) & \Omega_s^*\, e^{i\phi(t)}/2 \\ \Omega_p/2 & \Omega_s\, e^{-i\phi(t)}/2 & \delta_p + S_2 \end{bmatrix},$$

where the effective pump frequency Ω_p and the Stark shifts S_i are given by

$$\Omega_p = -\frac{\Omega_{p1}\Omega_{p2}^*}{2\delta_2}, \quad S_1 = -\frac{|\Omega_{p1}|^2}{4\delta_2}, \quad S_2 = -\frac{|\Omega_{p2}|^2}{4(\delta_2 - \delta_p)}.$$

Performing a unitary transformation gauging away $\delta_2(t)$ we finally obtain

$$\tilde{H}'_{ave} = \begin{bmatrix} 0 & 0 & \Omega_p^*/2 \\ 0 & \delta - (2S_1 + S_2) & \Omega_s/2 \\ \Omega_p/2 & \Omega_s/2 & \delta_p + (S_2 - S_1) \end{bmatrix}. \qquad (13)$$

This Hamiltonian has the standard structure of equation (11), apart for the Stark shifts S_i. Thus the three-tone drive could yield successful STIRAP also at the symmetry point, where the matrix elements Q_{01} and Q_{12} needed for coupling the two-pump field are large (see figure 4). The presence of the Stark shifts requires some care, since they produce large stray detunings, comparable with the amplitudes of the effective fields. In particular, since $\delta - [2S_1(t) + S_2(t)] \geqslant \Omega_p(t)$, coherent population transfer is suppressed even for $\delta = 0$ (see figure 5, top panel).

This drawback can be avoided by a suitable pulse shaping, a problem addressed in optimal control theory [33]. Indeed, the structure of the average Hamiltonian allows us to foresee a way to reduce the impact of pump-induced shifts by only reshaping the Stokes pulse. We assume equal pump pulse amplitudes, $\Omega_{p1}(t) = \Omega_{p2}(t)$, and we add an extra phase modulation to the Stokes pulse, $\phi'_s(t) = \int_0^t dt'\, 3|\Omega_{pi}(t)|^2/(4\delta_2)$. The resulting average Hamiltonian is a straightforward modification of equation (13), where $\Omega_s(t) \to \Omega_s(t)\, e^{-i\phi'_s(t)}$. Indeed, the dispersive condition means that $|\Omega_{pi}(t)|^2/\delta_2 \ll \delta_2 \ll \omega_k$, implying that the approximations leading to the RWA are still valid and that the new envelope is still slowly varying on the scale of δ_2 (inset of figure 5—the bottom panel), allowing us to rederive equation (13). At this stage a final transformation gauges away both Stark shifts, leading exactly to the standard form (11). Therefore, we expect a large efficiency, the critical requirement being $\delta \ll \Omega_p$. This expectation is confirmed by the numerical evaluation of the dynamics determined by the RWA Hamiltonian $\tilde{H}_p + \tilde{H}_s$ with the modulated Stark pulse (figure 5, bottom).

From the physical point of view, working at the symmetry point ensures that the decoherence due to low-frequency noise is strongly suppressed, still allowing large enough values of the effective $\Omega_p \sim |\Omega_{pi}|^2/\delta_2$. An appealing feature of devices such as the CPB and flux qubits is that both protection from noise and coupling to the drive improve for increasing values of E_J/E_C, contrary to what happens for conventional STIRAP at off-symmetry bias [29], due to the behavior of matrix elements $Q_{ij}(E_J/E_C)$ (see figure 4(b)). This favorable trend is, however, expected to weaken for larger and larger E_J/E_C, when the spectrum becomes nearly harmonic and the system may climb the ladder multilevel structure under the action of ac drives [32].

6. Conclusions

Superconducting circuits are a promising technology for the realization of quantum information on a solid-state platform.

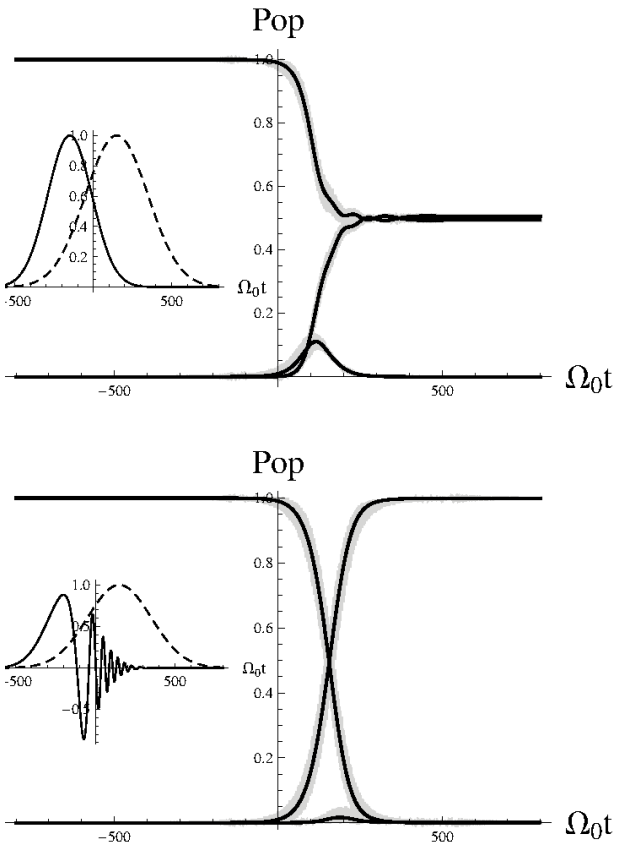

Figure 5. Exact population histories for a three-level system subject to a three-tone external drive (gray curves) are compared with the coarse-grained version (black lines) obtained by equation (13). The agreement of the average Hamiltonian approximation is excellent. Top: population histories for monochromatic pulses at nominal two-photon resonance $\delta = 0$, where stray Stark shifts prevent efficient STIRAP. Bottom: population histories with the phase corrected Stokes field (in the inset) which allows for faithful population transfer. Here the peak Rabi frequencies are $\Omega_s = \Omega_{p1} = \Omega_{p2} =: \Omega_0$, $\Omega_0 T = 200$ and $\delta_2 = 5\Omega_0$. The relevant figure for STIRAP is approximately $\sim \Omega_p T = 20$.

The design of several types of qubits [4] may allow us to fabricate novel architectures where new protocols of advanced quantum control by ac fields can be demonstrated. The ability to manipulate interference effects in multilevel artificial atoms even in the presence of low-frequency noise may open up an exciting perspective when coupling with electrical [7] or nanoelectromechanical [23, 34] resonators, where they may be used as switches or generate non-classical photon or phonon states, or used in hybrid platforms [10]. Interesting applications to quantum state processing have also been proposed such as the implementation of gates and memories using dressed states [35].

A general mathematical issue is that fluctuations in the properties of the device can be translated into equivalent fluctuations of the driving fields. Actually, from the physical point of view, decoherence due to the smaller resilience of artificial atoms has a counterpart in the fact that microwave sources needed for the latter are more stable than optical sources in atomic physics. This allows us to explore the fact that control fields have different limitations.

An interesting aspect emerging from this work is that as long as we consider slightly more complex architectures, such as three-level structures, the physical picture is enriched by qualitatively new phenomena. In this case the challenge is to find, if any, few relevant figures of merit which summarize the properties of quantum dynamics.

Note that Rabi spectroscopy could be richer in multilevel systems. For instance, oscillations between the ground and the second excited state of a superconducting nanocircuit may suffer large fluctuations $\delta Q_{20}(x)$ near the symmetry bias point, where $Q_{20} = 0$ vanishes due to selection rules. Since this coupling would be essential for the implementation of the conventional Lambda scheme (section 4), the observation of Rabi oscillations between these almost forbidden transitions would be an important step.

Finally, we note that from the technical point of view it is remarkable that adiabatic elimination performs so well (see figures 5) for STIRAP at the symmetry point, since the assumption of depopulated intermediate state of the usual derivation of the effective two-photon pump drive is not met during the central 'adiabatic passage' phase. We stress that, although sharing some similarity with the so-called chirped STIRAP [36], it is different since it is a sort of self-consistent and pulse-dependent optimization. We expect that a full numerical optimization [33, 37] will improve this part of the protocol further suppressing population of $|\phi_2\rangle$.

Acknowledgments

This work was partially supported by EU through grant no. PITN-GA-2009-234970, and by the joint Italian–Japanese Laboratory on 'Quantum Technologies: Information, Communication and Computation' of the Italian Ministry of Foreign Affairs.

Appendix. Parametric dependence of decay

The decay law equation (9) depends on the spectrum via the series expansion of $\Omega_{\rm fl}(x)$. We define the derivatives of the spectrum $A_i = \partial E_i/\partial q$ and $B_i = \partial^2 E_i/\partial q^2$ and the coefficients $a_{\rm R} = (\partial Q_{10}/\partial q)/Q_{10}$ and $b_{\rm R} = (\partial^2 Q_{10}/\partial q^2)/Q_{10}$ and expand

$$\delta(q+x) \approx \delta_0 + A_1(q)\,x + \tfrac{1}{2}\,B_1(q)\,x^2,$$
$$\Omega_{\rm R}(q+x) \approx \Omega_{\rm R0}\big[1 + a_{\rm R}(q)\,x + \tfrac{1}{2}\,b_{\rm R}(q)\,x^2\big].$$

This makes explicit the dependence on the parameters $(q, \Omega_{\rm R0}, \delta_0)$ which are taken as independent. We also define $(A_{\rm R}, B_{\rm R}) = \Omega_{\rm R0}(a_{\rm R}, b_{\rm R})$ which scales with $\Omega_{\rm R0}$; note that (A_1, B_1) scale with the much larger Bohr splitting. With this notation, coefficients entering equation (9) read

$$A(q, \Omega_{\rm R0}, \delta_0) = [\delta_0 A_1 + \Omega_{\rm R0} A_{\rm R}]/\Omega_{\rm fl},$$
$$B(q, \Omega_{\rm R0}, \delta_0) = [A_1^2 + A_{\rm R}^2 - A^2 + \delta_0 B_1 + \Omega_{\rm R0} B_{\rm R}]/\Omega_{\rm fl}.$$

At resonance they reduce to $A = A_{\rm R}$ and $B = A_1^2/\Omega_{\rm R0} + B_{\rm R}$, which would imply a Gaussian time decay if fluctuations of Q_{10} were important; otherwise the decay has essentially power-law behavior. In the dispersive regime we would have $A \approx A_1$, i.e. when energy fluctuations are linear we recover the Gaussian decay law of coherent oscillations, and $B \approx (B_1 + A_{\rm R}^2)/\Omega_{\rm fl}$.

References

[1] Nielsen M and Chuang I 2000 *Quantum Computation and Quantum Information* (Cambridge: Cambridge University Press)
[2] Chen G, Church D A, Englert B-G, Henkel C, Rohwedder B, Scully M O and Zubairy M S 2007 *Quantum Computing Devices: Principles, Designs and Analysis* (London: Chapman and Hall/CRC)
[3] Ladd T D, Jelezko F, Laflamme R, Nakamura Y, Monroe C and O'Brien J L 2010 *Nature* **464** 45
[4] Clarke J and Wilhelm F K 2008 *Nature* **453** 1031
[5] Falci G and Fazio R 2005 *Quantum Computer, Algorithms and Chaos* ed G Casati, D L Shepeliansky, P Zoller and G Benenti (Amsterdam: IOS Press) pp 363–416
[6] Paladino E *et al* 2009 *Phys. Scr.* **T137** 014017
[7] Schoelkopf R J and Girvin S M 2008 *Nature* **451** 664
[8] Scully M O and Zubairy M S 1997 *Quantum Optics* (Cambridge: Cambridge University Press)
[9] Grifoni M and Paladino E 2008 Focus on Quantum Dissipation in Unconventional Environments *New J. Phys.* **10** 115003
[10] Buluta I, Ashhab S and Nori F 2011 *Rep. Prog. Phys.* **74** 104401
[11] Vion D, Aassime A, Cottet A, Joyez P, Pothier H, Urbina C, Esteve D and Devoret M H 2002 *Science* **296** 886
[12] Paladino E *et al* 2010 *Phys. Rev.* B **81** 052502
Paladino E *et al* 2011 *New J. Phys.* **13** 093037
[13] D'Arrigo A and Paladino E 2012 *New J. Phys.* **14** 053035
[14] La Cognata A *et al* 2011 *Int. J. Quantum Inform.* **9** 1
[15] Ithier G *et al* 2005 *Phys. Rev.* B **72** 134519
[16] Nakamura Y *et al* 2002 *Phys. Rev. Lett.* **88** 047901
Astafiev O *et al* 2004 *Phys. Rev. Lett.* **93** 267007
Paladino E *et al* 2008 *Phys. Rev.* B **77** 041303
[17] Sank D *et al* 2012 *Phys. Rev. Lett.* **109** 067001
[18] Bylander J *et al* 2011 *Nature Phys.* **7** 565
[19] Chiarello F *et al* 2012 *New J. Phys.* **14** 023031
[20] Falci G, D'Arrigo A, Mastellone A and Paladino E 2005 *Phys. Rev. Lett.* **94** 167002
[21] You J Q and Nori F 2011 *Nature* **474** 589
[22] Murali K V R M, Dutton Z, Oliver W D, Crankshaw D S and Orlando T 2004 *Phys. Rev. Lett.* **93** 087003
Dutton Z *et al* 2006 arXiv:cond-mat/0604104
[23] Siewert J, Brandes T and Falci G 2006 *Opt. Commun.* **264** 435
Siewert J, Brandes T and Falci G 2009 *Phys. Rev.* B **79** 024504
[24] Mariantoni M *et al* 2005 arXiv:cond-mat/0509737v2
[25] Liu Y-X, You J Q, Wei L F, Sun C P and Nori F 2005 *Phys. Rev. Lett.* **95** 087001
[26] Mangano G, Siewert J and Falci G 2008 *Eur. Phys. J. Spec. Top.* **160** 259
[27] Bergmann K, Theuer H and Shore B W 1998 *Rev. Mod. Phys.* **70** 1003
[28] Vitanov N V, Fleischhauer M, Shore B W and Bergmann K 2001 *Adv. At. Mol. Opt. Phys.* **46** 55
[29] Falci G *et al* 2012 STIRAP in a Cooper Pair Box: low-frequency noise and design optimization in preparation
[30] Ivanov P A, Vitanov N V and Bergmann K 2004 *Phys. Rev.* A **70** 063409
[31] Haeberlen U and Waugh J S 1968 *Phys. Rev.* **175** 453
[32] Berritta M 2012 *PhD Thesis* University of Catania, Italy
[33] Zhu W and Rabitz H 1998 *J. Chem. Phys.* **109** 385
[34] Merlo M, Haupt F, Cavaliere F and Sassetti M 2008 *New J. Phys.* **10** 023008
Cuniberti G, Sassetti M and Kramer B 1998 *Phys. Rev.* B **57** 1515
[35] Timoney N, Baumgart I, Johanning M, Varon A F, Plenio M B, Retzker A and Wunderlich Ch 2011 *Nature* **476** 185
[36] Vitanov N V, Halfmann T, Shore B W and Bergmann K 2001 *Annu. Rev. Phys. Chem.* **52** 763
[37] Kumar P, Malinovskaya S A and Malinovsky V S 2011 arXiv:1104.4639